Uptake Rate Measurements of Methanesulfonic Acid and Glyoxal by Aqueous Droplets

Francis Schweitzer, Laurent Magi, Philippe Mirabel, and Christian George*

Centre de Géochimie de la Surface/Centre National de la Recherche Scientifique and Université Louis Pasteur, 28 rue Goethe, F-67083 Strasbourg, France

Received: July 28, 1997; In Final Form: November 3, 1997[⊗]

The uptake kinetics of methanesulfonic acid (CH_3SO_3H, MSA) and glyoxal (CHOCHO, ethanedial) by aqueous solutions were studied as a function of temperature using the droplet train technique combined with mass spectrometry and FTIR detection. The measured uptake kinetics for MSA were shown to be independent of the composition of the aqueous phase for NaCl concentrations in the range from 0 to 2 M. The mass accommodation coefficient was determined as a function of temperature between 261 and 283 K. The measured values decreased from 0.16 to 0.1 in this temperature range. The uptake kinetics of glyoxal were studied as a function of temperature between 263 and 283 K and were very close to our detection limit in pure water (i.e., uptake coefficient γ close to 10^{-3}) but were strongly affected by the pH (in the range from 1 to 14) or by sulfite ions (γ increasing to $\sim$0.02). The rate constant of the reaction between nonhydrated glyoxal and sulfite ions was determined to be $\sim 7.6 \times 10^6$ M^{-1} s^{-1} at 283 K. The mass accommodation temperature dependence was beyond the sensitivity of the technique employed in this study; therefore, we report an average value of $\alpha = 0.023$ for the studied temperature range. The uptake kinetics of CHOCHO were shown to be in agreement with bulk properties for temperatures larger than 273 K but deviate from it below. A surface reaction where glyoxal is protonated prior to accommodation was discussed as a possible explanation for an increased uptake rate in acidic solutions.

Introduction

A major task of interest within the field of tropospheric chemistry concerns a better characterization of its oxidation capacity, i.e., its ability to oxidize trace gases. It has been recognized recently that this oxidation capacity can be strongly affected by the occurrence of heterogeneous processes, due to the presence of atmospheric condensed matter. The uptake of trace gases by this condensed matter may increase or decrease the oxidation capacity depending on the nature of the species taken up. For example the uptake, by the liquid phase, of soluble species such as HO_2, H_2O_2 etc. may strongly inhibit the reactions taking place in the gas phase, which in turn corresponds to a slowing down of the oxidation capacity of the gas phase. Inversely, the uptake of reactants correspond to an increase of this oxidation capacity since the free radical concentrations may be increased by the lower concentrations of trace species. It is therefore crucial to understand how these gas/condensed matter exchanges proceed and to identify the corresponding chemistry.

In the marine boundary layer, the sulfur cycle dominates the gas to particle conversion and the growth of aerosols. This sulfur originates either from biogenic processes or from polluted air masses transported to the marine boundary layer.[1−3] In the biogenic processes, dimethyl sulfide (DMS) originates from bioactivity in phytoplankton, and since it is a poorly soluble gas, it is released to the gas phase where it is oxidized by either OH (during daytime) or NO_3 (during nighttime). Beside SO_2 and SO_3 (leading to the formation of H_2SO_4), stable products in the oxidation scheme of DMS have been identified to be dimethyl sulfoxide (CH_3SOCH_3, DMSO), dimethyl sulfone ($CH_3SO_2CH_3$, $DMSO_2$), and methanesulfonic acid (CH_3SO_3H, MSA).[4] All these products are more water soluble than DMS, and therefore it appears highly probable that phase partitioning takes place. Sulfuric and methanesulfonic acids are the main oxidation products leading to particle formation. In regard to the difference in their equilibrium vapor pressures, it is generally assumed that only H_2SO_4 nucleates homogeneously whereas MSA will only contribute to the growth of particles through condensation.[5] Once in the liquid phase, methanesulfonic acid may undergo H abstraction when reacting with several oxidants (OH, NO_3, ...) leading to the formation of H_2SO_4.[6] However, to understand to what extent MSA controls the condensationnal growth of particles and its role in wet chemistry, one has to know the parameters describing the efficiency of gas/liquid collisions, i.e., the mass accommodation coefficient.

Similar conclusions can be drawn for aldehydes that are generated in the atmosphere from the degradation of hydrocarbons.[7] It is now recognized that gas-phase aldehydes that are transferred into aqueous droplets are stabilizing agents for S(IV) in the sense that they lead to the formation of stable complexes. These latter are much less reactive toward the attack of free radicals and essentially inert against typical oxidants (i.e., O_3, H_2O_2).[8] Such processes have a direct impact on the H_2SO_4 formation rate and on the scavenging of SO_2 by cloud droplets. In fact, Olson and Hoffmann[8] have shown that the presence of glyoxal (CHOCHO) in aqueous droplets may double their content in sulfur. Such dicarbonyls have been identified in fog- and rainwater in concentrations up to 276 μM.[9] Munger et al.[9] have shown that approximately 50% of the glyoxal is partitioned to the aqueous phase during cloudy periods, which has to be compared with the 90% of formaldehyde remaining in the gas phase. In such a situation, the uptake of CHOCHO subsequently followed either by its hydratation or by the formation of stable

* Corresponding author. E-mail: george@illite.u-strasbg.fr.
⊗ Abstract published in *Advance ACS Abstracts,* December 15, 1997.

S1089-5639(97)02451-1 CCC: $15.00
Published on Web 01/15/1998

complex with S(IV) represents not only a reservoir for this latter but also for the aldehyde. Again, the knowledge of uptake kinetics is central for a better description of both gas and wet chemistry.

The rate at which a trace gas molecule may be transferred, from a well-mixed gas phase at a given concentration n_{mixed}, into the condensed phase can be obtained from the kinetic theory of gases. This allows the calculation of the maximum flux Φ_{max} that may cross the gas/liquid interface

$$\Phi_{max} = {}^1/_4\langle c\rangle n_{mixed}\alpha \quad (1)$$

where $\langle c\rangle$ is the trace gas average thermal velocity and α is the mass accommodation coefficient that characterizes the gas/liquid efficiency for the accommodation process. It represents the probability that a molecule, impinging on the interface, will be transferred into the condensed phase. However, eq 1 does not describe the overall uptake kinetics since it does not account for limitations introduced by diffusion processes (in both phases, i.e., gas and liquid), by saturation phenomena of the interface or by slow chemical transformation in the condensed phase. To take such limitations into account, one can extend eq 1 by introducing the uptake coefficient γ that allows the determination of the effective flux Φ_{eff} actually crossing the interface:

$$\Phi_{eff} = {}^1/_4\langle c\rangle n_{mixed}\gamma \quad (2)$$

In this equation, which is very similar to eq 1, α has been replaced by the uptake coefficient γ. This parameter can be defined as the probability that a striking molecule will be taken up by the condensed phase (similarly to α) but considering now the overall uptake process. Therefore, the uptake coefficient γ will be a function of the diffusion rates in both phases (described by their respective diffusion coefficients), of the accommodation process (described by the accommodation coefficient α), of the solubility (which depends upon the Henry's law constant H), and of the reactivity in the liquid phase (controlled by the rate constant). Therefore uptake rate measurements from the gas phase will provide useful information on such fundamental properties of the gas under study.

In the present work, we report uptake rate measurements for methanesulfonic acid and glyoxal using the droplet train technique. These studies have been performed as a function of temperature and initial composition of the droplets on which the uptake is measured. The results will lead to an increased level of knowledge for the accommodation process and reactivity of these species.

Experimental Section

Apparatus. The technique used to measure the uptake rates has already been described elsewhere,[10] and therefore we will only provide a brief summary of its principle of operation. The uptake coefficient is measured by the decrease of the gas-phase concentration of the trace species, due to the exposure to a monodisperse train of droplets. These latter are generated by a vibrating orifice (75 μm diameter) leading to droplet diameters in the range 80−150 μm.

The apparatus, where the contact between both phases takes place, is a vertically aligned flow tube which internal diameter is 1.8 cm. Its length can be varied up to 20 cm, to change the gas/liquid interaction time (0−20 ms) or the surface exposed by the droplet train (0−0.2 cm^2). Since the uptake process is directly related to the total surface S exposed by the droplets, any change ΔS in this surface results in a change Δn of the trace gas density at the exit ports of the flow tube. In fact, by considering the kinetic gas theory, it becomes possible to calculate the instantaneous uptake rate as:

$$\frac{dn}{dt} = -{}^1/_4\langle c\rangle n\gamma_{obs}\frac{S}{V} \quad (3)$$

where γ_{obs} is the experimental uptake coefficient and V the volume of the interaction chamber. However, since we are measuring the averaged signal during the transit time due to changes in the exposed surface**,** eq 3 has to be integrated leading to[11]

$$\gamma_{obs} = \frac{4F_g}{\langle c\rangle\Delta S}\ln\left(\frac{n}{n-\Delta n}\right) \quad (4)$$

where F_g is the carrier gas volume flow rate and n is the trace gas density before frequency or length switching. Typical experimental values for F_g are in the range 200−650 mL min^{-1} STP. By measuring the fractional changes in concentration $[n/(n-\Delta n)]$ as a function of $4F_g/(\langle c\rangle\,\Delta S)$, it becomes possible to determine the overall uptake coefficient γ_{obs}. This parameter can be measured as a function of the total pressure (for these experiments within the range 15−30 Torr), gas/liquid contact time or composition of the liquid used to produce the droplets. These last measurements are necessary to decouple the overall process into individual steps.

An important aspect of this technique is the careful control of the partial pressure of water in the flow tube since it controls the surface temperature of the droplets through evaporative cooling.[11] Therefore, the carrier gas (helium) was always saturated, at a given temperature, with water vapor before entering the flow tube. The equilibrium between ambient saturated helium and the liquid droplets is reached in the first zone of the setup before the interaction zone. The liquid used to produce the droplets was thermostated up to the orifice, for temperatures larger than 0 °C, leading to fast equilibrium attainment. Temperatures lower than 0 °C were obtained through evaporative cooling of the droplets in the first part of the flow tube. At these lower temperatures, the droplets are supercooled but not frozen even for temperatures lower than −20 °C.[11] However, for supercooled droplets the temperature refers to the surface thermal equilibration that occurs on a time scale of about 1ms and is therefore obtained before the droplets reach the region where they are exposed to the trace gases. Thermal conduction for our droplets has a characteristic time of about 10 ms meaning that although the surface quickly equilibrates with the ambient water vapor, the interior of the droplets' volume will not be at equilibrium. As shown by Worsnop et al.,[11] the measured uptake rate is therefore an average over a range up to 3 K around the desired temperature (including an uncertainty of 10% on the water partial pressure).

Gas Production and Analytical Methods. Aqueous solutions used to prepare the droplets were made from Milli-Q water (18 MΩ cm) and reagent-grade salts when necessary. MSA is commercially available from Aldrich with a minimum purity of 99% and was used without further purification. Because of its very low vapor pressure, a gas-phase stream was obtained by passing helium (purity >99.999%) into a bubbler containing MSA heated at 90 °C leading to a number density of about 10^{13} cm^{-3}. To maintain MSA in the gas phase, it was necessary to heat up all tubings and the flow tube at the same temperature, avoiding therefore cold points on which MSA would have been condensing. In such a situation the droplets' surface temperature is still governed by the ambient vapor pressure and not by the

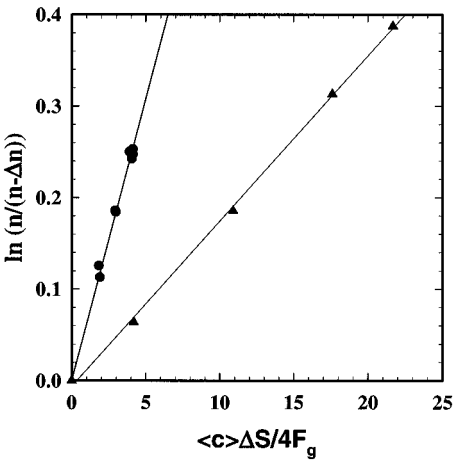

Figure 1. Typical plots of $\ln(n_{in}/n_{out})$ versus $\langle c\rangle\ \Delta S/4F_g$ for MSA on pure water (circles) and glyoxal on 1M NaOH (triangles) at 273 K according to eq 4. The slopes of such plots are a measure of the uptake coefficient γ. The solid line represents a linear fit to our data.

wall temperature as shown by De Bruyn et al.[12] In fact, since thermal diffusion is a slow process (within our time scale of a few milliseconds) it does not have time to affect the temperature of the droplets.

Glyoxal is also commercially available from Aldrich as a 40% aqueous solution where it exists primarily in its dihydrated form $(CH(OH)_2)_2$. To obtain the unpolymerized and water-free species,[13] the following procedure was used: ca. 20 mL of the aqueous solution was evaporated under vacuum until it gave an extremely dark and viscous liquid. This latter was then heated under vacuum, at least to 180 °C, to obtain a black and crispy residue. The gas phase evolving from this treatment was passed subsequently through traps containing calcium sulfate and diphosphorus pentoxide. The chemicals at the output of these traps were collected at liquid nitrogen temperature. The analysis, by FTIR and mass spectrometry, of the vapor of this product showed pure nonpolymerized glyoxal.

An ion-trap mass spectrometer (Varian model Saturn 4D) and a FTIR spectrometer (Nicolet Protégé 460 equipped with an IRA long-path White-cell; light path ranging from 2.2 to 22 m) were connected to the exit ports of the flow tube. The gas-phase concentration of MSA was monitored by the signal (integrated over 1s) at *m*/*e* 79, i.e., the major peak in its mass spectra when ionized at 70 eV. Glyoxal was analyzed by FTIR and especially by following the evolution of its absorption band at 2844 cm^{-1}. Infrared spectra were taken in the range 4000−400 cm^{-1} and were coadded in order to increase the S/N ratio. The detection limits were approximately 10^{11} and 10^{12} molecules cm^{-3} for the mass and FTIR spectrometers, respectively.

Results and Discussion

As already mentioned, uptake coefficients are measured from the fractional changes in trace gas concentration due to a modification of the total surface exposed by the droplets. Figure 1 shows typical data obtained for both MSA and glyoxal, plotted according to eq 4. The slope of the fitted line represents the uptake coefficient γ_{obs}, which is a measure of the net flux crossing the gas/liquid interface. As we already mentioned, it is therefore a function of the diffusion rates in both phases, of the accommodation process, of the solubility, and of the reactivity in the liquid phase. To each of these processes, one can attribute a specific uptake coefficient according to[14]

$$\text{diffusion limitation:}\quad \frac{1}{\gamma_{diff}} = \frac{\langle c\rangle d_{eff}}{8D_g} - \frac{1}{2} \tag{5}$$

$$\text{saturation limitation:}\quad \gamma_{sat} = \frac{8HRT\sqrt{D_a}}{\langle c\rangle\sqrt{\pi t}} \tag{6}$$

$$\text{reactivity limitation:}\quad \gamma_{rxn} = \frac{4HRT\sqrt{kD_a}}{\langle c\rangle} \tag{7}$$

where d_{eff} is the effective droplet diameter (which takes into account the fact that a droplet train may not be considered as a sum of individual droplets; note however that its value is very close to the real diameter),[11] H is the Henry's law constant, R is the perfect gas constant, T is the temperature, D_g and D_a are the gas and aqueous phase diffusion coefficients, t is the gas/liquid contact time, and k is the first-order rate constant for a given reaction in the liquid phase. The overall uptake coefficient can be calculated by summing up the individual resistances (defined as the inverse of the specific uptake coefficient) according to[14]

$$\frac{1}{\gamma} = \frac{1}{\gamma_{diff}} + \frac{1}{\alpha} + \frac{1}{\gamma_{sat} + \gamma_{rxn}}$$

$$= \frac{\langle c\rangle d_{eff}}{8D_g} - \frac{1}{2} + \frac{1}{\alpha} + \frac{\langle c\rangle}{4HRT\sqrt{D_a}}\left(\frac{2}{\sqrt{\pi t}} + \sqrt{k}\right)^{-1} \tag{8}$$

This relation clearly shows that the uptake coefficient is a function of different fundamental properties of the molecule such as solubility, diffusion, etc. The treatment used to obtain eq 8 is very similar to the one used for the calculation of deposition velocity on the ocean surface.[15]

Table 1 gives the data needed in order to apply eq 8, i.e., the diffusion coefficient in both phases and Henry's law constant. For both species, diffusion coefficients are not known and have therefore been estimated using methods presented by Reid et al.[16] Especially, the semiempirical calculations by Fuller et al.[17] were applied for gas-phase mass transport. In addition, since our carrier gas is a mixture of helium and water vapor, it is necessary to know the diffusion in this background. This is done according to the following equation

$$\frac{1}{D_g} = \frac{P_{H_2O}}{D_{g-H_2O}} + \frac{P_{He}}{D_{g-He}} \tag{9}$$

where D_g is the diffusion coefficient in the mixed background, P_{H_2O} and P_{He} are the partial pressures of water and helium respectively, and D_{g-H_2O} and D_{g-He} are the binary diffusion coefficients of the trace gases in water and helium, respectively. The employed estimation method has an average absolute error of about 5%,[16] which will, under our experimental conditions, introduce an additional error of less than 5% in the measured mass accommodation coefficients. Note, however, that this error will only apply for MSA, for which the uptake kinetics are sufficiently large so that diffusion corrections become important. Correspondingly, aqueous phase-diffusion coefficients have been estimated using the method developed by Wilke and Chang[18] with a typical error of about 11%[16] when considering diffusion in water, leading to a 5% error in the reported product $H\sqrt{k}$.

Methanesulfonic Acid. MSA is highly soluble in water where its physical Henry's law constant is 8.7×10^{11} M atm^{-1}; i.e., MSA is nearly infinitely soluble in water.[19] In such a

TABLE 1: Binary Diffusion Coefficients in Helium and Water Vapor, Aqueous Phase Diffusion Coefficients, and Henry's Law Constant for MSA and Glyoxal[a]

	D_{X-H_2O}[b] ($cm^2\ s^{-1}$)	D_{X-He}[b] ($cm^2\ s^{-1}$)	D_{aq}[c] ($cm^2\ s^{-1}$)	H ($M\ atm^{-1}$)
CH_3SO_3H (MSA)	0.13	0.37	1.2×10^{-5}	8.7×10^{11}[d]
CHOCHO (glyoxal)	0.16	0.44	1.6×10^{-5}	5.0[e]

[a] All values are reported at 298 K. Gas-phase diffusion coefficients are expected to follow a $T^{1.75}$ dependency, whereas aqueous-phase diffusion coefficients are assumed to follow a T/η law where η is the viscosity of the solvent. the Henry's law constant dependence with T is unknown for both species, but for glyoxal it was assumed to be the same as for formaldehyde. [b] Method developed by Fuller et al.[17] as given by Reid et al.[16] [c] Method developed by Wilke and Chang[18] as given by Reid et al.[16] [d] Brimblecombe et al.[19] [e] See text. Estimated from the hydration constant and the effective Henry's law constant.

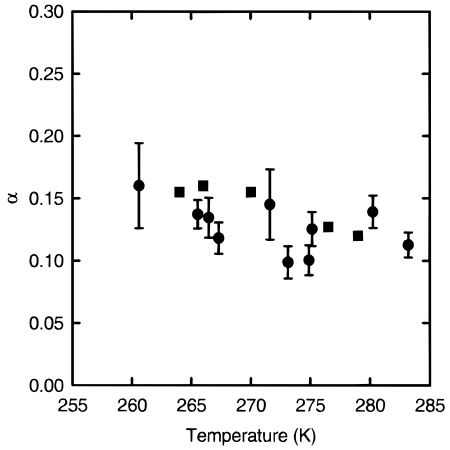

Figure 2. Plot of α versus temperature for methanesulfonic acid exhibiting a negative temperature dependence. The error bars are given at the 2σ level. (Circles, this work; squares, De Bruyn et al.[12])

situation, the resistance due to the saturation of the interface does not play any role, and the flux crossing the interface should be time-independent. We verified experimentally that the uptake coefficient is indeed time-independent between 5 and 15 ms confirming that γ_{sat} is negligible at all temperatures compared to the other resistances. We also modified the composition of the droplets by adding NaCl with concentrations ranging from 0 to 2 M. Even in the more concentrated solutions, we could not see any differences in the uptake kinetics. This is easily understood when taking into consideration the enormous solubility of MSA in water. In fact, any molecule of MSA that is transferred across the barrier represented by the interface will be taken up irreversibly. In such a case, eq 8 can be simplified as

$$\frac{1}{\gamma} = \frac{\langle c \rangle d_{eff}}{8D_g} - \frac{1}{2} + \frac{1}{\alpha} \tag{10}$$

where only the resistance introduced by gas-phase diffusion and the accommodation steps have been retained. Figure 2 shows the mass accommodation coefficients obtained, as a function of temperature, once the uptake coefficients have been corrected for diffusion limitations using eq 10. The α values exhibit a clear negative dependency with temperature, the values decreasing from 0.16 to 0.1 for temperatures increasing from 261 to 283 K. Figure 2 also shows the excellent agreement with the previously published results obtained by De Bruyn et al.[12] leading to an increased level of confidence in the reported mass accommodation coefficients in both studies.

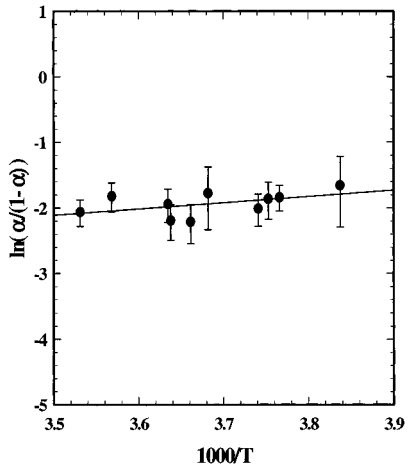

Figure 3. Representation of $\ln(\alpha/1-\alpha)$ versus $1/T$ according to eq 11 for methanesulfonic acid. The solid line represents a linear fit to our data, and its results given value of $\Delta H^{\ddagger}_{obs}$ and $\Delta S^{\ddagger}_{obs}$. The error bars are given at the 2σ level.

To describe the observed negative temperature dependence, several authors have considered that mass accommodation can be viewed as a multistep process where the trace gas first thermally accommodates on the droplet surface, with unit probability, and remains adsorbed until it undergoes a further step into the liquid or until it is released back to the gas phase. Davidovits *et al.*[20] hypothesized that the rate-limiting step in the mass accommodation is part of the physical solvation process. Therefore, the transition from the gas phase into the liquid phase can be summarized as[21]

$$n_g \underset{k_{desorb}}{\overset{k_{ads}}{\rightleftharpoons}} n_s \xrightarrow{k_s} n^*_s \xrightarrow{k_{sol}} n_l \tag{11}$$

where the subscripts g, s, and l refer to the gas, surface, and liquid state of the trace gas. Since the interface is a dynamic region where water clusters are formed and destroyed continuously, the solvation process is expected to involve the formation of liquidlike clusters. As in classical theory of nucleation, only cluster reaching a critical size (n^*_s in eq 11) may grow indefinitely and finally merge with the nearby liquid. The critical size N^* is defined as the number of molecules in the cluster or more precisely the number of hydrogen bonds used to form the cluster. Then any cluster taken up by the liquid consists of $N^* - 1$ water molecules. The mass accommodation coefficients therefore reflect the competition between the rate of solvation (k_{sol}) and especially of cluster formation (k_s, which is proportional to k_{sol}) and desorption (k_{desorb}) of the surface species. By considering this model, the flux of molecules crossing the interface (eq 1) can be rewritten as

$$^1/_4\langle c \rangle n_g \alpha = {}^1/_4\langle c \rangle n_g - n_s k_{desorb} = n_s k_{sol} \tag{12}$$

By considering that both k_{sol} and k_{desorb} can be expressed by an Arrhenius exponential temperature dependence relationship, eq 12 can be rearranged, leading to:

$$\ln\left\{\frac{\alpha}{1-\alpha}\right\} = -\frac{\Delta G^{\ddagger}_{obs}}{RT} \tag{13}$$

where $\Delta G^{\ddagger}_{obs}$ can be regarded as the height of the Gibbs free energy barrier between the gas and the surface transition state. The enthalpy ΔH_{obs} and entropy ΔS_{obs} can be derived from a plot of $\ln(\alpha/1-\alpha)$ versus $1/T$ as displayed in Figure 3. The

TABLE 2: Measured Values for the Enthalpy ΔH_{obs} and Entropy ΔS_{obs} for the Accommodation Process for Methanesulfonic Acid

	ΔS_{obs} (cal mol^{-1} K^{-1})	ΔH_{obs} (kcal mol^{-1})
this work	-14.0 ± 3.1	-2.7 ± 0.7
De Bruyn et al.[12]	-16.7 ± 2.2	-3.5 ± 0.6

slope of such a plot corresponds to $-\Delta H_{obs}/R$, while the intercept corresponds to $\Delta S_{obs}/R$. The values obtained for ΔS_{obs} and ΔH_{obs} are summarized in Table 2 along with those measured by De Bruyn et al.[12] Again, the comparison between both studies is excellent.

It is clear that this Gibbs energy $\Delta G^{\ddagger}_{obs}$ is related to fundamental properties of the trace gas and especially to its ability to form hydrogen bonds with water. These latter are, in fact, central to the formation of the liquidlike clusters. Davidovits et al.[20] and Nathanson et al.[21] demonstrated a direct relationship between ΔH_{obs}, ΔS_{obs}, and the size of the critical cluster governed by N^*. Therefore this latter parameter can be determined from the values of the enthalpy and entropy given in Table 2. Our measured values are found to agree with this formulation with a critical size $N^* \sim 1.5$. This noninteger value may be regarded as an average size between clusters consisting of MSA alone and clusters with MSA and one water molecule. It must be noted that the N^* value for MSA is very low compared to other reported values. This can probably be explained by the expected very high H-bonding ability of MSA due to the presence of several oxygen on the sulfur leading to several bonding sites, but also to an increasing of the polarity of the S−O covalent bonds thus increasing the strength of the weak hydrogen bonds.[12] The same kind of observation may hold for H_2SO_4 whose accommodation coefficient is not yet known.

The values of α reported here are quite large, i.e., 0.1 or larger. It could therefore be interesting to know whether mass accommodation may play a role in the condensational growth of particles due to the uptake of MSA. This can be done using the theoretical description of uptake kinetics provided by Schwartz,[22] who gives expressions of the maximum rate at which a gas species may transferred into a condensed phase by homogeneous diffusion and interfacial transport. This latter depends on the magnitude of the accommodation coefficient, whereas diffusion rate depends upon the diffusion coefficients and the size of the aqueous droplets. Figure 4 shows a comparison of both rates as a function of droplets' size and mass accommodation coefficients. It appears that for MSA, the transport may be limited by gas-phase diffusion when considering the uptake by small droplets, i.e., with diameters smaller than 1 μm. Since it is expected that MSA is involved in the condensational growth of particles, it is therefore highly probable that the initial steps of such processes are limited by mass accommodation. We therefore recommend that modeling studies based upon particle growth in the sulfur cycle treat the accommodation step in detail.

Glyoxal. Aldehydes are known to react with water to give stable gem-diols.[23] In the case of glyoxal, this hydration process consists of two steps, according to the following scheme:

$$CHOCHO_{aq} + H_2O \leftrightarrow CH(OH)_2CHO \qquad K_1 \quad (14)$$

$$CH(OH)_2CHO + H_2O \leftrightarrow CH(OH)_2CH(OH)_2 \qquad K_2 \quad (15)$$

The occurrence of such equilibria greatly affects the solubility of glyoxal since they increase the quantity of aldehydes that may be dissolved in water. To take these equilibria into account,

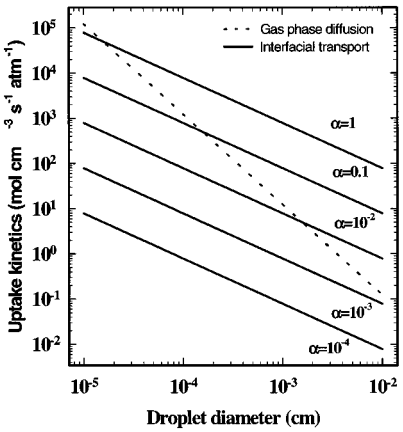

Figure 4. Comparison the maximum transfer rates, for methanesulfonic acid, due to gas-phase diffusion and interfacial mass transport according to the work of Schwartz. This figure shows that the transport across the gas/liquid interface may be limited by interfacial transport for small droplets (diameters smaller than 1μm).

one can define an effective Henry's law constant as

$$H^* = \frac{[CHOCHO_{aq}] + [CH(OH)_2CHO] + [CH(OH)_2CH(OH)_2]}{[CHOCHO_g]} \quad (16)$$

where the subscripts g and aq refer to the gaseous and aqueous state for glyoxal. This equation can be rearranged in the form

$$H^* = H(1 + K_1 + K_1K_2) \quad (17)$$

where H is the physical Henry's law constant. However, most of the constants needed here are unknown; i.e., we could not find in the open literature values for H, K_1, K_2 and for the rate of achievement of the equilibria 14 and 15. Nevertheless, Zhou and Mopper[24] measured the effective solubility of glyoxal at 298 K to be 3.6×10^5 M atm^{-1} in agreement with the lower limit of 3 10^5 M atm^{-1} reported by Betterton and Hoffmann.[25] Other studies were found that focus mostly on the hydration constant for glyoxal.[26−28] These experimental investigations could only concern the global hydration process, i.e., the following equilibrium:

$$CHOCHO + 2H_2O \leftrightarrow CH(OH)_2CH(OH)_2 \qquad K_{hyd} \quad (18)$$

The reported values for K_{hyd} (or for the product K_1K_2) are very large, i.e., on the order of 10^5, but they differ nearly by an order of magnitude. Nevertheless, all these studies agree with the fact that glyoxal is predominantly present in the aqueous phase as dihydrated, meaning that eq 17 can be simplified to

$$H^* = HK_{hyd} \quad (19)$$

By considering a recent determination of K_{hyd} by Montoya and Mellado[28] who reported $K_{hyd} = 7.22 \times 10^4$, we estimated the physical solubility of glyoxal as

$$H \sim 5 \text{ M atm}^{-1} \text{ at } 298 \text{ K} \quad (20)$$

Since in this work we are concerned with uptake rate measurements as a function of temperature, we had to estimate the T dependence of H and K_{hyd}. Such a dependence has already been reported for formaldehyde for both constants,[25,26] and we simply

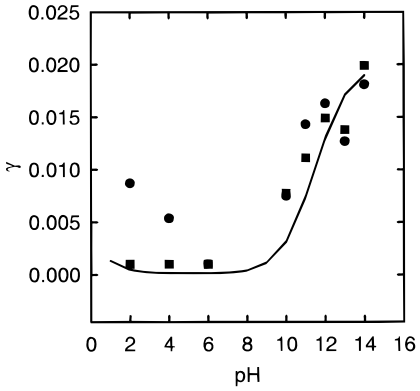

Figure 5. Uptake coefficient for glyoxal as a function of pH at 268 K (circles) and 278 K (squares). The solid line represents a model of the uptake coefficient based on estimated bulk properties. At the lower temperature, a deviation from the expected behavior (solid line) is observed.

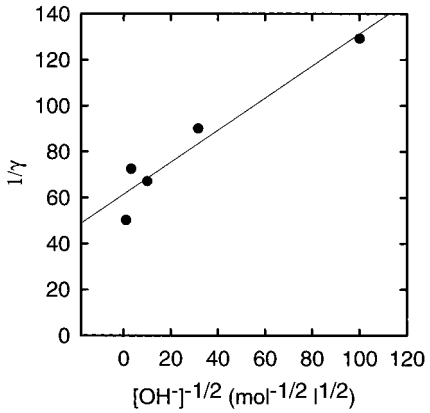

Figure 6. Plot of $1/\gamma$ versus $[OH^-]$ at 278 K according to eq 19 for glyoxal. The solid line represents a linear fit to our data. The slope of such a fit yield value of $H\sqrt{k}$, while the intercept is a measure of the mass accommodation coefficient.

assumed that the same variations apply to glyoxal, which is similar in nature to CH_2O.

The estimated Henry's law constant (eq 20) is nearly four times larger than that for formaldehyde[25] but still remains small. Therefore, the uptake by pure water may be very limited if the hydration reactions do not occur within the time scale of our experiments (i.e., a few milliseconds). In fact, using eq 8 we calculated the uptake coefficient associated with the physical solubility of glyoxal (i.e., γ_{sat}) to be $\leq 2 \times 10^{-3}$ for temperatures between 283 and 263 K within our experimental time scale (5−20 ms). Such a value is very close to our detection limit, i.e., $\gamma \geq 10^{-3}$, and we were in fact unable to obtain reliable data for the uptake rate on pure water at all temperatures. In regard to the low solubility of glyoxal, this feature is not unexpected, and we can simply report that γ is close to 10^{-3} on pure water. This observation means that physical solubility cannot account for large uptake rates for CHOCHO.

The gem-diol formation is generally acid and base-catalyzed[29] and such a catalysis was indeed reported for glyoxal.[27] In such a situation, the uptake rate may be enhanced by the presence of H^+ or OH^- ions. As shown in Figure 5, we observed an enhancement of the uptake rate in alkaline solutions at all temperatures but only an acid catalysis at temperatures lower than 273 K. This observation is proof that the uptake of glyoxal is governed by its reactivity. Therefore, eq 8 can be simplified to

$$\frac{1}{\gamma} \approx \frac{1}{\alpha} + \frac{\langle c \rangle}{4HRT\sqrt{kD_a}} \qquad (21)$$

where the influences of gas-phase diffusion and saturation of the interface are omitted. Since no reliable data have been published on the bulk hydration kinetics of glyoxal, we have to consider that the kinetics reported for formaldehyde is applicable to the system we consider in this study. Schecker and Schulz[30] studied the hydration kinetics of formaldehyde and reported the following first-order rate constant:

$$k = 7.8 \times 103 \exp\left(\frac{-15\,868}{RT}\right) \times (1 + 870[H^+] + 6.3 \times 10^6[OH^-]) \qquad (22)$$

where R is in SI units. Using this equation and the estimated Henry's law constant, it becomes possible to calculate the dependence of γ with pH as shown in Figure 5 by the solid line. Despite all the assumptions made, the agreement between this simple calculation and our measurements is reasonably good for all pH values at temperatures larger than 273 K. But below this threshold temperature, the agreement is only valid for pH values larger than 6, meaning that this simple model cannot account for the observed acid catalysis at low temperature. As shown by eq 21, our calculations need the knowledge of α, which was obtained from the intercept of a plot of γ^{-1} vs $[OH^-]^{-1/2}$ (Figure 6). The values we obtained were only poorly temperature-dependent, and we could not extract any trend in opposition to what was found for MSA. As a result, we can only report that the mass accommodation coefficient for glyoxal is between 0.034 and 0.016 for temperatures in the range from 263 to 283 K with an average value of 0.023. These values for α are the first determination for this parameter but compare very favorably with the estimates reported[31] for formaldehyde, i.e., 0.02, and for acetaldehyde i.e., larger than 0.03. It should be noted that for these two aldehydes the temperature dependence of α could not be measured. This arises probably from the fact that the uptake rate is governed by the reactivity of the aldehyde meaning that the second term of the right-hand side of eq 21 dominates the temperature dependence. Finally, it should be noted that the model for mass accommodation shortly presented above is only valid for gases with a large intrinsic solubility, which is not the case for glyoxal.

As already noted, eq 21 which is based on bulk properties, cannot explain the measured uptake in acidic solutions at low temperature. We believe that this discrepancy between our calculations and the experimentally determined kinetics is not due to an incorrect estimate of the temperature dependence of H or k. In fact, the hydration rate is not expected to increase at low temperature, and a large Henry's law constant would affect all the data in the complete pH range and not only for pH values lower than 4. It is therefore possible that this deviation from bulk kinetics is due to a surface effect. Such observations have already been made for SO_2,[11] $ClONO_2$,[32] $ClNO_2$,[33] and other aldehydes.[31,34] Jayne et al.[31] reported that the uptake kinetics of acetaldehyde is enhanced by the formation of a surface complex inducing a time dependence in the measured uptake coefficient, in a manner similar to bulk saturation of the droplet's surface, but now attributed to the very narrow interface. However, we were not able to identify any time dependence of γ within our experimental time scale. We therefore believe that the increased uptake originates from another process, i.e., a surface reaction with H^+. Jayne et al.[31] and Tolbert et al.[34]

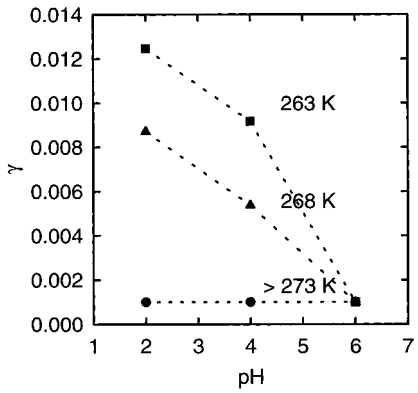

Figure 7. Variation of the uptake coefficient of glyoxal in acidic solutions exhibiting an increasing uptake rate at low temperature. This latter is attributed to a surface reaction.

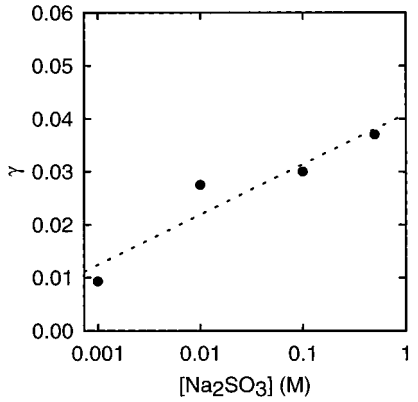

Figure 8. Influence of the sulfite ions concentration on the uptake rate of glyoxal. The increase of the values of γ is significant of a direct reaction between nonhydrated glyoxal and SO_3^{2-}.

demonstrated that formaldehyde can effectively be protonated at the surface of very acidic liquids but also at pH $\sim$ 2 leading to an increased uptake at low temperature. Since formaldehyde and glyoxal are species of similar nature, we believe that the same assumption holds for CHOCHO. The observed temperature dependence (Figure 7) can be understood by considering that any trace gases first thermally stick on the surface of the droplet until it undergoes a next step, which could correspond to the accommodation or chemical reaction. At low temperature, we could expected that the residence time on the surface increases leading to a favored chemical reaction. To quantitatively describe this surface kinetics, more precise measurements are needed that could specifically interrogate the surface state of glyoxal (for example with second harmonic generation), which is far beyond the actual ability of our droplet train technique. Nevertheless, we tried to apply a model derived from an Eley−Rideal mechanism by Hu et al.[35] where a surface uptake coefficient is introduced as

$$\gamma_{surf} = \frac{a[H^+]}{1 + b[H^+]} \qquad (23)$$

where the constants *a* and *b* are related to the surface reactivity of glyoxal. In the pioneer work of Hu et al.[35] these constants were different, but the evidence of surface reaction we obtained is not strong enough to give enough insight to the system. Therefore, we approximated both constants to be equal. This new uptake coefficient can be interconnected in the resistance model used to obtain eq 8 as

$$\gamma = (1 - \gamma_{surf})\gamma_{bulk} + \gamma_{surf} \qquad (24)$$

where γ_{bulk} is defined by eq 21 and where the limitations introduced by slow gas-phase diffusion were omitted. Using the mass accommodation values derived from alkaline solutions, we fitted this equation to our acid catalysis. The values we obtained for *a* (and *b*) are 1.14 $\pm$ 0.62 and 0.77 $\pm$ 0.35 at 263 and 268 K, respectively. The addition of a new step in the resistance model greatly enhances the agreement between experiments and modeling. We believe, despite the fact that our very simple description of the reactivity of glyoxal in acidic solutions at low temperature probably did not capture all the details of this process, that some nonbulk chemistry is occurring, which we attributed to a surface reaction as this was done for formaldehyde.[31,36]

Since in the real atmosphere the chemistry of glyoxal and S(IV) can be interconnected, we also studied the influence of SO_3^{2-} on the uptake kinetics. Sulfite ions are known to react reversibly with nonhydrated glyoxal according to[23]

$$CHOCHO + SO_3^{2-} \rightarrow CHOCH(O^-)SO_3^- \qquad (25)$$

which can be followed by the formation of a bidisulfite adduct. However, for our droplet train studies only the first step, i.e., the reaction between nonhydrated glyoxal and sulfite ions is accessible. As can be seen from Figure 8, the addition of SO_3^{2-} enhances the uptake rate. These ions were dissolved as Na_2SO_3 at pH = 9 in order to maintain all S(IV) as sulfite and to avoid any influence of the OH^- catalysis. By fitting eq 21 to our data, we can access the rate constant for reaction 25. The rate constants we determined are 5.8×10^6 and 7.6×10^6 M^{-1} s^{-1} at 263 and 283 K, respectively. These values can be favorably compared to the apparent rate constants reported by Olson and Hoffmann, who could not follow directly the kinetics of nonhydrated glyoxal.

Conclusion

In this paper, we reported uptake studies using the droplet train technique for methanesulfonic acid and glyoxal. For the acid, we determined the values of the mass accommodation coefficient as a function of temperature. The observed negative temperature is in agreement with a model where accommodation is a dynamic process occurring in the very narrow region defining the interface. Using the values of α, we conclude that the transport across the gas/liquid interface may be limited by interfacial transport for small droplets (diameters smaller than 1 μm). Since MSA is involved in the condensational growth of particles, it becomes probable that the initial steps of such processes are limited by mass accommodation. We therefore recommend that modeling studies based upon particle growth in the sulfur cycle treat the accommodation step in detail.

Concerning glyoxal, we determined that the uptake kinetics for temperatures larger than 273 K are in agreement with bulk properties and exhibit a base-catalyzed hydration process. We also measured the rate constant of the reaction between nonhydrated glyoxal and sulfite ions. This constant is sufficiently large that this reaction may effectively play a role in atmospheric chemistry by providing a pathway where both glyoxal and S(IV) are retained in stable complexes leading to an enrichment of sulfur in the atmospheric aqueous phase but also to a slowing down of the oxidation rates of S(IV). The mass accommodation coefficient of glyoxal is apparently independent of the temperature and is in the range where interfacial mass transport may play a very significant role even for droplets sizes up to 10 μm in diameter. At low temperatures

(<273 K), the uptake kinetics deviate from bulk properties since an increasing acid catalysis was observed. We speculate that it corresponds to a surface reaction where glyoxal is protonated prior to accommodation in agreement with other studies on formaldehyde.

Acknowledgment. This research was supported by the European Commission within the project RINOXA2 under the contract ENV4-CT95-0175.

References and Notes

(1) Wakeham, T. J.; Dacey, J. W. H. *ACS Symp. Ser*. **1989**, *393*, 152.
(2) Charlson, R. J.; Lovelock, J. E.; Andrae, M. O.; Warren, S. G. *Nature* **1987**, *326*, 655.
(3) Schwartz, S. E. *Nature* **1988**, *336*, 441.
(4) Barone, S. B.; Turnipseed, A. A.; Ravishankara, A. R. *Faraday. Discuss*. **1995**, *100*, 39.
(5) Kreidenweis, S. M.; Seinfeld, J. H. *Atmos. Environ*. **1988**, *22*, 283.
(6) Such studies are currently undertaken within the EU Project "Removal and Interconversion of Oxidants in the Atmospheric Aqueous Phase, Part 2", Acronym: RINOXA2. Zellner, R.; Herrmann, H.; Mirabel, Ph.; Buxton, G.; Salmon, A.; Sehested, K.; Holcman, J.; Rolle, W.; Brede O. Contract ENV4-CT95-0175, April 1996.
(7) Finlayson-Pitts, B. J.; Pitts, J. N., Jr. *Atmospheric Chemistry: Fundamentals and Experimental Techniques*; John Wiley & Sons: New York, 1986.
(8) Olson, T. M.; Hoffmann, M. R. *Atmos. Environ*. **1989**, *23*, 985.
(9) Munger, J. W.; Jacob, D. J.; Daube, B. C.; Horowitz, L. W.; Keene, W. C.; Heikes, B. G. *J. Geophys. Res*. **1995**, *100*, 9325.
(10) Magi, L.; Schweitzer, F.; Pallares, C.; Cherif, S.; Mirabel, Ph.; George, Ch. *J. Phys. Chem.*, in press.
(11) Worsnop. D. R.; Zahniser, M. S.; Kolb, C. E.; Gardner, J. A.; Watson, L. R.; Van Doren, J. M.; Jayne, J. T.;. Davidovits, P. *J. Phys. Chem*. **1989**, *93*, 1159−1172.
(12) De Bruyn, W. J.; Shorter, J. A.; Davidovits, P.; Worsnop, D. R.; Zahniser, M. S.; Kolb, C. E. *J. Geophys. Res*. **1994**, *99*, 16927.
(13) Gurnick, M.; Chaiken J.; Benson, Th.; McDonald J. D. *J. Chem. Phys*. **1981**, *74*, 99.
(14) Kolb, C. E.; Worsnop, D. R.; Zahniser M. S.; Davidovits, P.; Hanson, D. R.; Ravishankara A. R.; Keyser, L. F.; Leu, M. T.; Williams, L. R.; Molina, M. J.; Tolbert, M. A. *Laboratory Studies of Atmospheric Heterogeneous Chemistry*; Current Problems in Atmospheric Chemistry; Barker, J. R., Ed.; Advances in Physical Chemistry Series; World Scientific Publishing Co.: Singapore, 1994.
(15) Liss, P. S.; Slater, P. G. *Nature* **1974**, *247*, 181.
(16) Reid, R. C.; Prausnitz, J. M.; Poling B. E. *The Properties of Gases and Liquids*, 4th ed.; McGraw-Hill Inc.: New York, 1987.
(17) Fuller, E. N.; Ensley, K.; Giddings, J. C. *J. Phys. Chem*. **1969**, *75*, 3679.
(18) Wilke, C. R.; Chang, P. *AIChE J*. **1955**, *47*, 1253.
(19) Brimblecombe, P.; Clegg, S. L. *J. Atmos. Chem*. **1988**, *7*, 1.
(20) Davidovits, P.; Jayne, J. T.; Duan, S. X.; Worsnop, D. R.; Zahniser, M. S.; Kolb, C. E. *J. Phys. Chem*. **1991**, *95*, 6337.
(21) Nathanson, G. M.; Davidovits, P.; Worsnop, D. R.; Kolb, C. E. *J. Phys. Chem*. **1996**, *100*, 13007.
(22) Schwartz, S. E. *Chemistry of Multiphase Atmospheric Systems*; NATO ASI Ser., 4, 415; Jaeschke, W., Ed.; Springer-Verlag: Berlin Heidelberg, 1986.
(23) Olson, T. M.; Hoffmann, M. R. *J. Phys. Chem*. **1988**, *92*, 533.
(24) Zhou, X; Mopper, K. *Environ. Sci. Technol*. **1990**, *24*, 1864.
(25) Betterton, E. A.; Hoffmann, M. R. *Environ. Sci. Technol*. **1988**, *22*, 1415.
(26) Bell, R. P. *Adv. Phys. Org. Chem*. **1966**, *4*, 1.
(27) Wasa, T.; Musha, S. *Bull. Univ. Osaka Prefect., Ser. A* **1970**, *19*, 169.
(28) Montoya, M. R.; Mellado, J. M. R. *Port. Electrochim. Acta* **1995**, *13*, 299.
(29) Ahrens, M. L.; Maass, G.; Schuster, P.; Winkler, H. *J. Am. Chem. Soc*. **1970**, *92*, 6134.
(30) Schecker, H. G.; Schulz G. *Z. Phys. Chem. (Munich)* **1969**, *65*, 221.
(31) Jayne, J. T.; Duan, S. X.; Davidovits, P.; Worsnop, D. R.; Zahniser, M. S.; Kolb, C. E. *J. Phys. Chem*. **1992**, *96*, 5452.
(32) Hanson, D. R.; Ravishankara, A. R. *J. Phys. Chem*. **1994**, *98*, 5728.
(33) George, Ch.; Behnke, W.; Scheer, V.; Zetzsch, C.; Magi, L.; Ponche, J. L.; Mirabel, Ph. *Geophys. Res. Lett*. **1995**, *22*, 1505.
(34) Tolbert, M. A.; Pfaff, J.; Jayaweera, I.; Prather, M. J. *J. Geophys. Res*. **1993**, *98*, 2957.
(35) Hu, J. H.; Shi, Q.; Davidovits, P.; Worsnop, D. R.; Zahniser, M. S.; Kolb, C. E. *J. Phys. Chem*. **1995**, *99*, 8768.
(36) Jayne, J. T.; Worsnop, D. R.; Kolb, C. E.; Swartz, E.; Davidovits, P. *J. Phys. Chem*. **1996**, *100*, 8015.